



Scale dependency of anisotropic thermal conductivity of heterogeneous geomaterials

Kai-Qi Li^{1,2} · Qi-Min Chen¹ · Guan Chen^{1,3}

Received: 7 December 2022 / Accepted: 6 February 2024 / Published online: 16 February 2024
© The Author(s) 2024

Abstract

The precise determination of subsurface thermal properties is critical for ground-source heating systems. The geomaterials are inherently heterogeneous, and their thermal conductivity measured in laboratory and field tests often exhibits anisotropic behaviours. However, the accurate measurement of thermal responses in geomaterials presents a challenging task due to the anisotropy's variation with the observed scale. Hence, a numerical method is developed in this work and illustrated by taking a typical anisotropic structure of geomaterials with the porosity of 0.5 as an example. The differences in data from laboratory measurements and field tests are discussed to explore the scale effect on anisotropic thermal properties. A series of simulation tests are conducted on specimens with varying dimensions using the finite element method. Results indicate that the thermal properties show a substantial sensitivity to the observation scale, the variation of which decreases with the sample dimensions. By comparing in situ data and laboratory results, the values of average thermal conductivity and corresponding anisotropy ratio are lower than those at small scales, indicating that careful consideration should be given to the thermal properties to account for heterogeneity and anisotropy. In addition, four upscaling schemes based on the averaging method are discussed. This study sheds light on the gap between the laboratory results and the field's inherent properties and provides guidelines for upscaling small-scale results to field-scale applications.

Keywords Scale dependency · Thermal conductivity · Heterogeneous geomaterials · Anisotropy · Statistical volume element · Upscaling method

Introduction

Geomaterials are heterogeneous, and their thermal properties tend to be anisotropic, both of which vary with scale (Samadhiya et al. 2008; Li et al. 2020; Rodriguez-Dono

et al. 2023). The anisotropic behaviour of geomaterials can be attributed to various factors, such as depositional processes and the existence of pores and/or cracks (Mitchell and Soga 2005; Zhang et al. 2022; Li et al. 2023c), and heterogeneity is the primary source of anisotropy (Lake 1988; Nie et al. 2023). The sedimentary processes within a formation can lead to evident stratification, and the properties of geomaterials in the horizontal direction differ from those in the vertical direction (Journel and Huijbregts 1978; Ghysels et al. 2018; Yang et al. 2021). Thermal conductivity of geomaterials (k) is an essential property of geomaterials, which plays a vital role in many geoengineering fields such as oil shale mining, exploitation of geothermal energy and optimal design of radioactive waste repository (Prats and O'Brien 1975; Rapti et al. 2022; Li et al. 2023a). Table 1 presents several typical experiments on the anisotropic thermal conductivity of heterogeneous geomaterials, including rock, clay, quartz sands and silts. It can be noted that a large number of studies on this topic have been explored, but they mainly focused on exploring the anisotropy of thermal

✉ Guan Chen
guan.chen@irz.uni-hannover.de

Kai-Qi Li
kqcee.li@polyu.edu.hk

Qi-Min Chen
chenqm2020@whu.edu.cn

¹ State Key Laboratory of Water Resources Engineering and Management, Wuhan University, Wuhan, Hubei 430072, People's Republic of China

² Department of Civil and Environmental Engineering, The Hong Kong Polytechnic University, Hung Hom, Kowloon, Hong Kong, China

³ Institute for Risk and Reliability, Leibniz Universität Hannover, 30167 Hannover, Germany

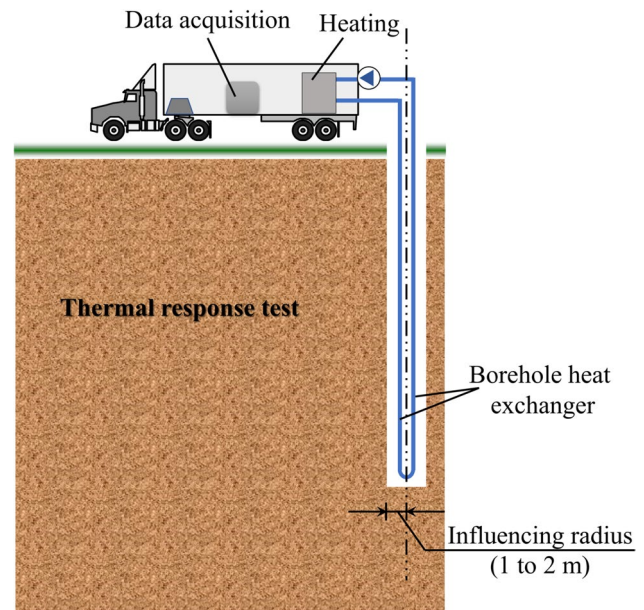
Table 1 Summary of typical investigations on the anisotropy in thermal properties of heterogeneous geomaterials

Materials	References
Rock	Čermák and Rybach 1982 (muscovite); Grubbe et al. 1983; Deming 1994; Schön 1996; Popov et al. 1999; Davis et al. 2007 (metasedimentary); Mehmani et al. 2016 (shale); Yu et al. 2023 (Tamusu mudstone)
Rock and clay	Penner 1963; Midttømme et al. 1997
Quartz sand and silts	Midttømme and Roaldset 1998
Clay	Midttømme et al. 1998; Buntebarth 2004; Mügler et al. 2006; Dao et al. 2014; Zhang et al. 2019

properties through experiments with limited sample dimensions (see Table 1).

An accurate evaluation of the thermal properties of geomaterials is also challenging. The thermal conductivity of geomaterials under different conditions (e.g. dry condition, saturated condition) varies from 0.1 to 7.8 W/(mK) (Côté and Konrad 2009; Liu et al. 2022), which can be affected by different factors such as mineralogy, density, water content, porosity, saturation and temperature (Brigaud and Vasseur 1989; Cho et al. 2009; Huang et al. 2023; Li et al. 2023b). Many scholars have discussed the sensitivity of those factors in relation to k through test and simulation methods. As for laboratory tests, the samples collected from drilling cores and outcrops are measured via steady-state or transient methods (Elkholy et al. 2019). The thermal response test (TRT) is a reliable approach to assess in situ thermal responses, particularly for applying the ground-coupled heat pump (GCHP), but it is relatively uneconomical.

Laboratory investigation on samples taken from boreholes is helpful in determining the thermal conductivity within a small scale (e.g. mm and cm) (Tarnawski et al. 2013), while TRT can reflect the thermal properties of geomaterials within a radius of influence of 1 to 2 m (see Fig. 1). The discrepancy can be observed between different scales, that is, scale dependence. Jorand et al. (2013) reported that the values of k from laboratory measurements are higher than those determined at a larger scale. Some scholars (Di Sipio et al. 2014; Blázquez et al. 2017; Haffen et al. 2017) have also attempted to map the thermal conductivity distribution of the earth's crust according to limited test data since it is likely to be impossible to measure all samples at the site of interest. For homogenous media, this type of upscaling strategy may not yield biases. However, this operation can result in significant deviations in the assessment of thermal conductivity over a much larger scale (e.g. regional scale) since the anisotropic nature of the thermal properties of heterogeneous geomaterials is scale-dependent. Furthermore, some determinations of the thermal conductivity of geomaterials have neglected its intrinsic heterogeneity and anisotropy in thermal properties (Popov et al. 2016). Therefore, investigations into how the thermal properties (i.e. thermal conductivity and anisotropy) of heterogeneous geomaterials

**Fig. 1** Schematic diagram of TRT (modified from Corcoran et al. 2019)

vary with the observed scale are essential for developing a feasible and eligible upscaling method from measurements of k at small scales to larger scales.

Due to the limited availability of anisotropic experimental samples of geomaterials and the scarcity of corresponding laboratory measurements (Vasseur et al. 1995), it is crucial to develop an effective method of analysing the scale dependence of anisotropy in thermal conductivity. Accordingly, the numerical technique is an appealing method to estimating the thermal properties of geomaterials with known internal structures (Wang et al. 2006). The quartet structure generation set (QSGS) method is employed to construct in situ geomaterial samples from TRT, which is acknowledged to be capable of characterising the porous structure of soils (Germanou et al. 2018). The reconstructed sample with the porosity of 0.5 serving as a representative of the TRT specimen is subsequently decomposed into $M \times M$ grids sample, since the anisotropy in thermal conductivity is closely associated with porosity and reaches its maximum

value at a porosity of 0.5 (Li et al. 2022). To investigate the scale dependency of thermal properties and their anisotropy ratio, various samples with different dimensions are extracted from the initial reconstructed TRT sample and analysed using the finite element method (FEM). The corresponding results of thermal properties and anisotropy ratio are recorded for further discussion. To explore the links between k values at different scales, four typical averaging approaches are also compared. This study presents the first effort to construct a simple framework that discusses the variation in anisotropic thermal properties with respect to observed scale, which sheds light on the gap between laboratory measurements and in situ properties and provides guidelines for upscaling geomaterials' properties in engineering.

Methodology

Existing prediction method for k

As a complex multiphase medium, evaluating the thermal conductivity of geomaterials is a challenging task. Various prediction models have been established based on limited laboratory data. One of the most widely used models for predicting k was proposed by Johansen (1977). Combining two conditions of geomaterials (i.e. dry and saturation state), this model can be extended to a wide range of water content.

$$k = (k_{\text{sat}} - k_{\text{dry}}) \times K_r + k_{\text{dry}} \quad (1a)$$

$$K_r = a \log S_r + 1 \quad (1b)$$

where K_r is normalised thermal conductivity which is the function of saturation; k_{sat} and k_{dry} are the thermal conductivity of geomaterials at dry and saturation states, respectively; a is an empirical parameter; and S_r is saturation degree. As a simple and easy-to-use model, Eq. (1) yields great performance for predicting k and has been referenced in many scientific studies (Balland and Arp 2005; Côté and Konrad 2005; Farouki 1981). Hence, the two extreme soil conditions above will be considered in further detail below for more general applications. Referring to Li et al. (2020), the thermal conductivity of solid (k_s), air (k_a) and water (k_w) is set to 4, 0.02 and 0.5 W/(mK), respectively.

Numerical method

The reconstruction technique adopted to rebuild the structure of geomaterials is first introduced in the following section. In addition, the calculation procedure for the thermal properties of heterogeneous materials is briefly elucidated.

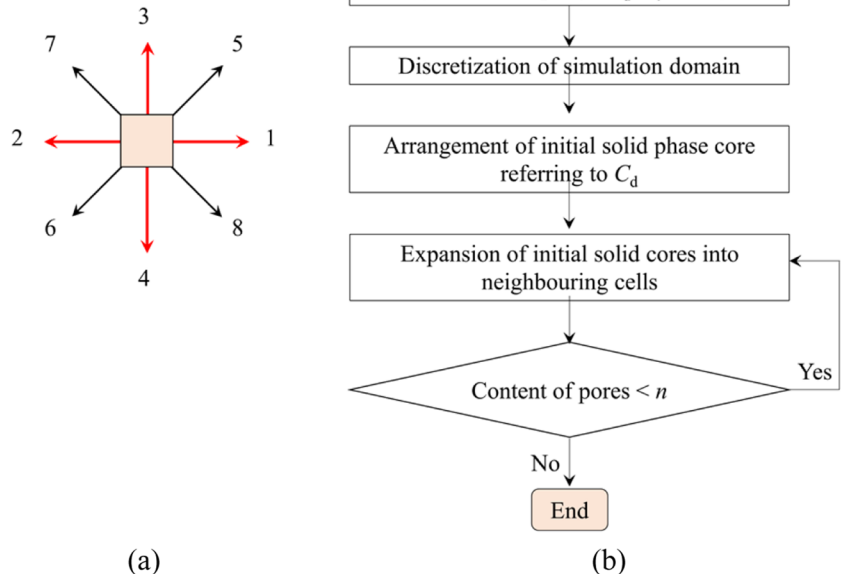
Reconstruction of geomaterials

Reconstruction of the anisotropic structure where solid fabrics exhibit preferred orientations is the key to determining the thermal conductivity of geomaterials. Jorand et al. (2013) reported that the anisotropy of geomaterials derives from three primary sources that are solid fabric configurations, orientations of flaws (e.g. cracks) and crystal anisotropy. In this work, we mainly focus on the influence of arrangements of solid fabrics on thermal behaviour and utilise the quartet structure generation set method to reconstruct the anisotropic structure of geomaterials. The reconstruction technique was initially proposed by Wang et al. (2007) and has been demonstrated to accurately replicate the morphology of natural soil specimens (Wang et al. 2017; Zhou et al. 2019). The effectiveness of this approach has also been validated by Li et al. (2022) and Han et al. (2023) to analyse the anisotropic thermal conductivity of geomaterials.

The reconstruction procedure involves four modelling parameters. The first parameter is the distribution probability of solid particle core (C_d), which controls initial solid core content placement. Other solids are generated based on the growth probability of solid (P_i) that contains four primary directions ($i = 1, 2, 3, 4$) and four secondary directions ($i = 5, 6, 7, 8$) (see Fig. 2a). The generation process of the solid phase will be terminated when the porosity (n) reaches the target content. Figure 2b demonstrates the flow chart of the whole modelling procedure. The anisotropic structure of geomaterials can be achieved by altering the value of P_i . When P_i in four primary directions is quadrupled that in four secondary directions, the rebuilt sample can be regarded as isotropic. As geomaterials tend to exhibit layering in the horizontal direction, the ratio of P_i in the x -direction to that in the y -direction, labelled “ Y ”, often exceeds 1.

Referring to Li et al. (2022), the heterogeneous geomaterials reconstructed with higher values of Y exhibit more pronounced layered structures, which in turn enhances the anisotropic effect in thermal conductivity. Thus, the critical modelling parameter “ Y ” is set as 50 in this work. In addition, Li et al. (2022) also indicated that the anisotropy ratio is closely related to porosity. More precisely, r_k increases initially and then decreases with increasing porosity, reaching its maximum if n equals 0.5. Since different geomaterials represent various combinations of factors (e.g. porosity and different levels of layered structure), we selected a geomaterial specimen whose $Y = 50$ and $n = 0.5$ as a typical example to investigate the scale dependency of thermal properties. Findings from this particular case can be used to predict thermal conductivity and the corresponding anisotropy ratio for other heterogeneous geomaterials with different structures in practice.

Fig. 2 Schematic diagram: (a) eight growth directions of solid core in QSGS method; (b) flowchart of the QSGS method to reconstruct the anisotropic geomaterials



Computation of thermal properties

We are interested in calculating the thermal responses of geomaterials at various dimensions and distinguishing their differences, especially the gap between data obtained from TRT and laboratory measurements. This typical sample from TRT is hereafter named “Sample T ”. A representative realisation of anisotropic geomaterial generated using the QSGS method is presented in Fig. 3, with the size of 2000 mm \times 2000 mm, which is consentient with the in situ TRT sample size. Three scales are involved in this study, i.e. in situ sample length (L), mesoscale length (L_m) that represents the size of the sample in centimetre and millimetre (e.g. laboratory-scale) and the minimum scale (d) that is the grid cell size used in the simulations and is equivalent to the solid size.

The representative volume element (RVE) is often employed to determine material properties (Hill 1963; Nie et al. 2021), the dimension of which is not fixed and depends on the specific property of interests. Statistical volume element (SVE) is typically implemented as an alternative to RVE, whose properties are variable from one sample to another. Therefore, for exploring the influence of observed scale on the anisotropy of thermal properties, the whole in situ specimen (i.e. sample T) is divided into $M \times M$ grids as depicted in Fig. 3 where every grid serves as an SVE. Herein, various samples with different dimensions (i.e. each grid in sample T) are extracted from sample T , defined as “sample S ”, and their corresponding thermal properties will

be calculated to explore the scale dependence of thermal conductivity.

For determining the thermal properties of SVE, a homogenisation procedure is conducted coupled with the finite element method (see Fig. 4). Thermal conductivity controls the heat transfer in geomaterials, the determination of which is based on Fourier’s law.

$$q = -k\nabla T \quad (2)$$

where q is the heat density, k represents the thermal conductivity and ∇T is the temperature gradient. Equation 2 is solved to simulate this steady-state thermal issue by applying the following boundary conditions:

Dirichlet boundary (uniform temperature boundary)

$$T = T_0 \quad (3)$$

The Dirichlet boundary condition denotes two opposite sides are imposed constant temperature to generate a temperature gradient.

Neumann boundary (adiabatic boundary)

$$\nabla T \cdot \mathbf{n} = 0 \quad (4)$$

where T_0 is a prescribed temperature; \mathbf{n} is the outward normal vector to the simulation domain. Each sample S is loaded with the defined two boundaries for homogenisation in the finite element analyses. When calculating the thermal conductivity along x -direction (k_x), the Dirichlet boundary is applied on the boundaries perpendicular to the horizontal

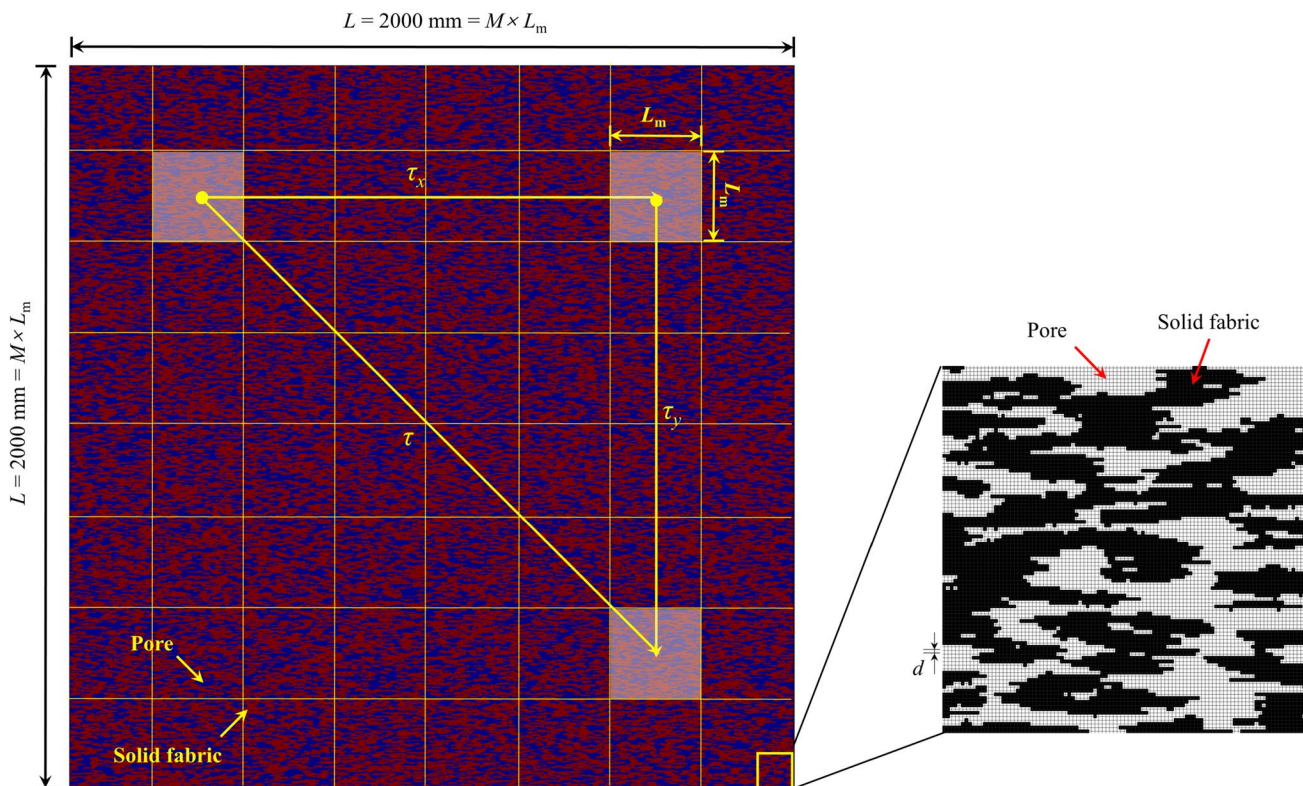


Fig. 3 Schematic diagram of simulation sample via QSGS method ($n=0.5$; $C_d=0.01$; $Y=50$) involving three scales (in situ scale L , investigation scale L_m and minimum grid scale d). The square with the length of L_m represents the investigation sample (i.e. sample S) where L_m varies

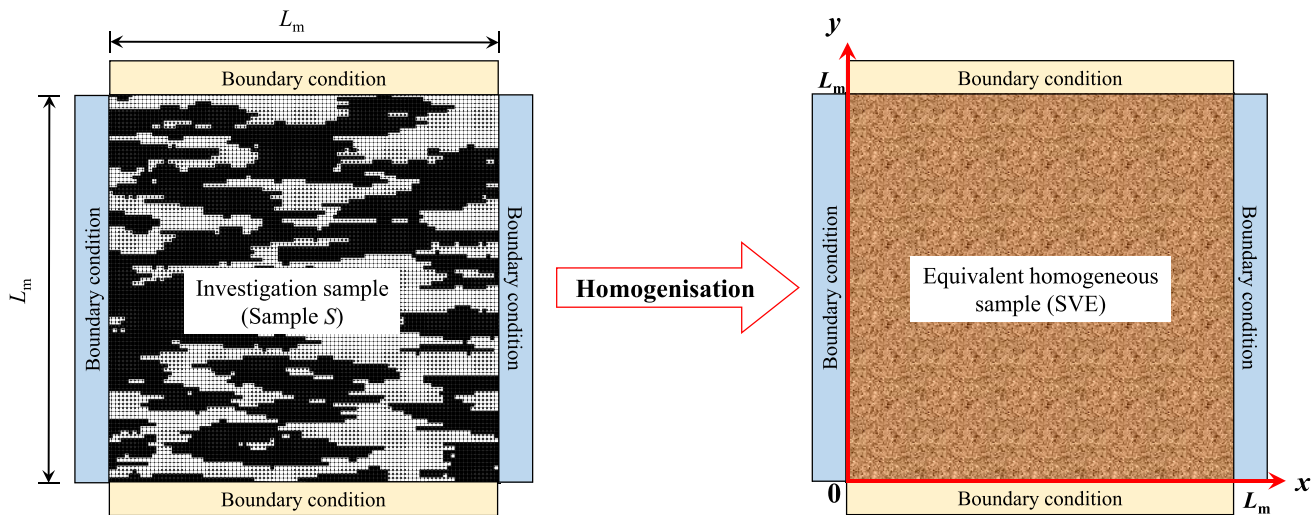


Fig. 4 Illustration of the homogenisation scheme. Boundary conditions refer to the Dirichlet or Neumann boundaries

direction and the Neumann boundary is set at the surfaces parallel to the x -axis. In contrast, the two boundary conditions are swapped if the value of thermal conductivity along y -direction (k_y) is needed to be computed.

As for the anisotropy in thermal conductivity, the anisotropy ratio (r_k) is defined as the ratio of the thermal conductivity in

the x -direction (k_x) to that in the y -direction (k_y) since the geomaterials possess apparent layered structures in the horizontal direction (Jung et al. 2021).

$$r_k = k_x/k_y \tag{5}$$

Results and discussion

Anisotropic structure of geomaterials

The Feret diameter, which was initially proposed by Walton (1948), is employed in this study to quantitatively characterise the horizontal layered features of solids in geomaterials. To assess the extent of the anisotropic structure of sample *T*, the rose diagram of angles between the Feret diameter and *x*-axis is plotted in Fig. 5. It seems that most of the minimum Feret diameter lies in the vertical direction, while the angle of maximum diameters ranges from 170 to 190°. Figure 5 indicates that reconstructed sample *T* has noticeable layered features, which echoes the modelling parameter *Y* with a higher value.

To shed light on the scale dependency on anisotropic thermal properties, all sample *S* (i.e. SVE) extracted from sample *T* are computed by Eqs. (2–5). Table 2 lists all the cases involved in our framework. Regarding laboratory measurements, the sample dimension is dependent on the specific testing methods employed. Typically, the specimen diameter should exceed 70 mm, and the minimum thickness should be no less than 90 mm. In this study, a typical sample dimension of 100 × 100 mm was used as a substitute for laboratory testing. It can be observed from Table 2 that the number of SVE that need to be calculated increases as the dimension of sample *S* reduces. In the following section, we will investigate the relationship between sample dimension and the thermal conductivity of geomaterials, as well as its corresponding anisotropy ratio. By conducting comprehensive experiments and analysis, the variations in thermal conductivity and anisotropy ratio across different sample dimensions will be elucidated.

Scale dependency on thermal properties

The thermal properties of each SVE are computed via FEM. Figure 6 depicts the results of r_k of dry sample *S* under three

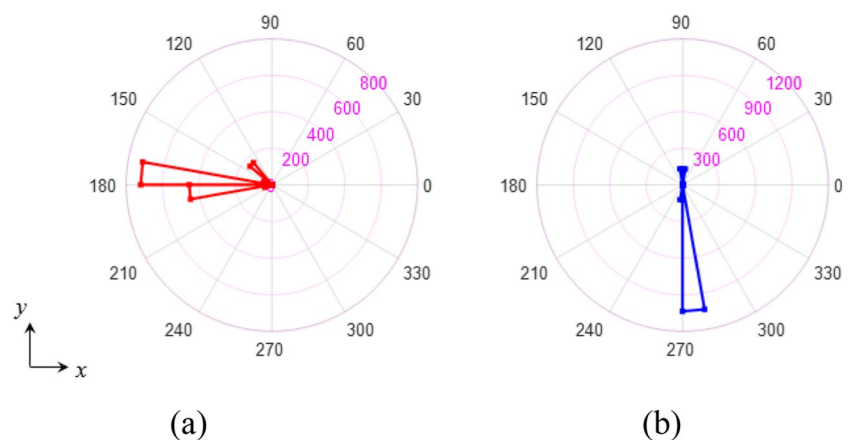
Table 2 Various sample dimensions of sample *S* considered in this study

Dimension of sample <i>S</i> (mm)	Number of sample <i>S</i>
2000 × 2000	1
1000 × 1000	4
500 × 500	16
400 × 400	25
250 × 250	64
100 × 100	400
50 × 50	1600
25 × 25	6400

typical dimensions (25, 100 and 400 mm). Results in Fig. 6a indicate that the range of the anisotropy ratio expands as sample *T* is gradually refined. As shown in Fig. 6b, the mean value of r_k increases from 7.9 to 17.75 as decreasing sample dimension. In addition, the anisotropy ratio tends to be distributed in a normal distribution form as sample *S* refines. All samples with different dimensions extracted from sample *T* are prepared and tested to determine the specific relationship between thermal properties and observed scales. The FEM results of eight cases in Table 2 are discussed in detail.

Figure 7 illustrates the simulation results marked with scatters, including the thermal conductivity in two orthogonal directions and the anisotropy ratio of various samples with different dimensions at dry conditions. The median, extremes, upper and lower quartiles are also shown with box-plot. The mean values of thermal properties in samples with the same dimensions are also represented in Fig. 7 by dashed lines. It can be noted that the curves of thermal properties (i.e. k_x , k_y and r_k) versus sample dimension by using mean value and median value exhibit similar trends. When the observed scale is relatively small, the properties in heat conduction have significant fluctuation. This can be attributed to the heterogeneity of the sample

Fig. 5 Rose diagram of (a) directional angle of the maximum Feret diameter with respect to *x*-axis; (b) directional angle of the minimum Feret diameter with respect to *x*-axis



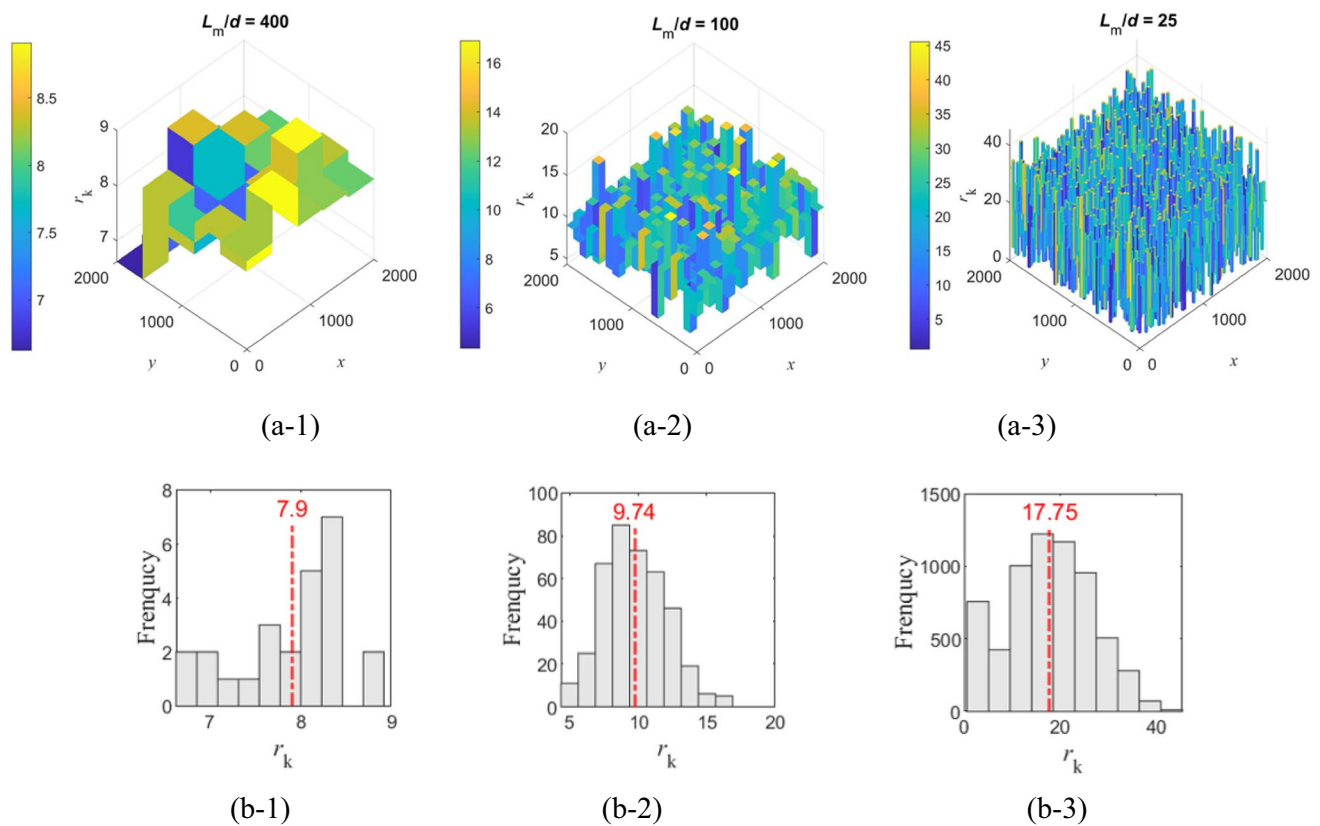


Fig. 6 Anisotropy ratios for dry geomaterials at three typical dimensions: **(a)** r_k of each SVE; **(b)** histogram of r_k

at a small scale inducing the heat transfer barriers or the flow channels with high connectivity. Both the average values of k_x and r_k have a similar trend as the increment of L_m/d . In particular, the anisotropy ratio can reach up to 45 when the observed scale is $25 L_m/d$. On the contrary, the r_k of sample T is 7.52, which is considerably lower than the datum at a small scale. The difference between data at small scales and results measured in situ tests demonstrates that direct upscaling of the results from small scales to large scales of interest in practical applications may lead to significant errors. Figure 7b also shows that the mean value of k_y hardly changes with the sample dimension, which can be attributed to sample S with horizontal layered structures so that the mean thermal transfer along the vertical direction is not sensitive to the sample dimension. Comparing those data, one can conclude that the variation in thermal conductivity of SVE decreases with the increasing observed scale. It should be emphasised that when upscaling the small-scale (e.g. laboratory-scale) experimental or numerical tests on the geomaterial samples to field scale, the anisotropy in thermal conductivity may be altered by the scale dependency.

As for sample S in a saturated state, similar results are also demonstrated in Fig. 8. In general, the comparison of the dotted and dashed curves in Fig. 8 illustrated

that the mean values of thermal conductivity and anisotropy ratio against sample dimension are consistent basically with the trends of median values of thermal properties with sample dimension. Some violent fluctuations of thermal conductivity and anisotropy ratio can be observed when the size of sample S is less than $250 L_m/d$. Unlike dry geomaterials, the discrepancy of average thermal responses between different scales is not as apparent for saturated samples, implying a slight decrease when the sample dimension increases. This can be attributed to the different ratios of thermal conductivity of solids to that of pores (k_s/k_p). For dry geomaterials, the ratio of k_s to k_a is equal to 200 ($= 4/0.02$), while the ratio of k_s to k_w is merely equal to 8 ($= 4/0.5$) when the sample is saturated. A higher ratio of k_s/k_p can promote the effect of heterogenous structure on the anisotropy in thermal conduction. According to previous analyses, the thermal behaviours of geomaterials in practice probably lie between the results of two extreme conditions of geomaterials.

Variation of thermal property

In this section, the scale dependency on thermal properties is explored by statistical analyses. For SVEs under the same

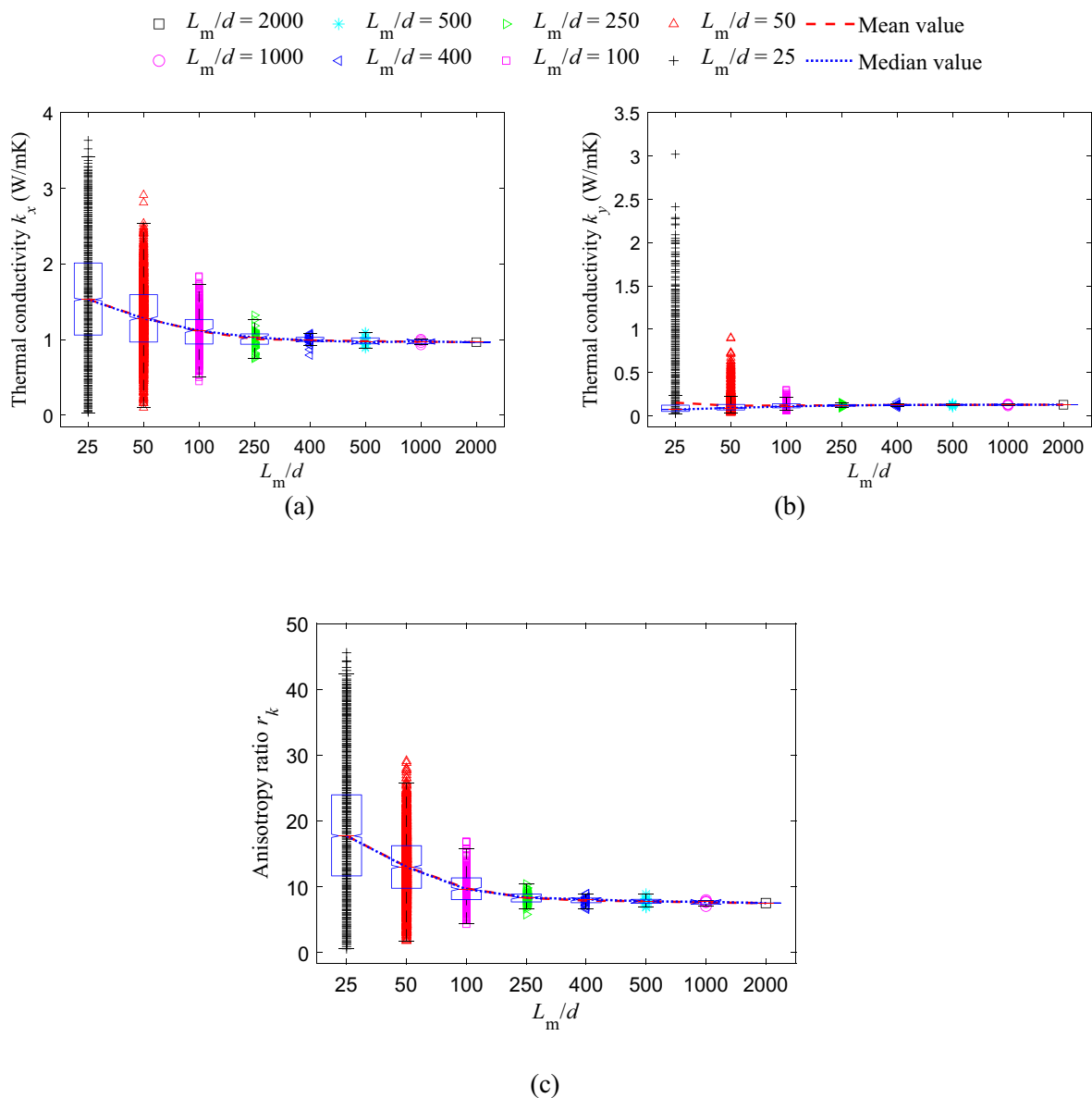


Fig. 7 Box plots of thermal properties of SVE at different scales for geomaterials at dry state: (a) thermal conductivity k_x ; (b) thermal conductivity k_y ; (c) anisotropy ratio r_k

dimension, their thermal conductivity and corresponding anisotropy ratio are recorded and utilised as inputs.

Figure 9 depicts the statistical convergence of the mean value and coefficient of variation (COV, which equals the ratio of standard deviation to mean) for sample S with different dimensions at dry and saturation conditions. In general, the mean values of thermal conductivities (i.e. k_x and k_y) of saturated samples with the same sample dimension are higher than those of dry samples since k_w is larger than k_a . The mean values of thermal properties of saturated samples do not present remarkable changes with L_m/d . However, the thermal conductivity of dry samples has more obvious scale-dependent characteristics (see Fig. 9a-1 to a-3). The greater

ratio of thermal conductivity ($k_s/k_p = 200$) leads to more considerable changes in mean values of k_x and r_k but smaller than that of k_y . The COV reduction is considerable when upscaling from a small scale to in situ scale, given in Fig. 9b.

Regarding the coefficient of variation (COV) of thermal conductivity, both dry and saturated samples exhibit a similar trend. The COV (k_x and k_y) decreases dramatically at relatively small scales where the sample dimension at dry conditions ranges from 25 to 250 L_m/d . When the observed scale is larger than 250 L_m/d , the COV has dropped to zero nearly. When the pores are occupied with water in geomaterials, the variation of COV in thermal conductivity is slight, ranging from 0.1 to 0 as L_m/d

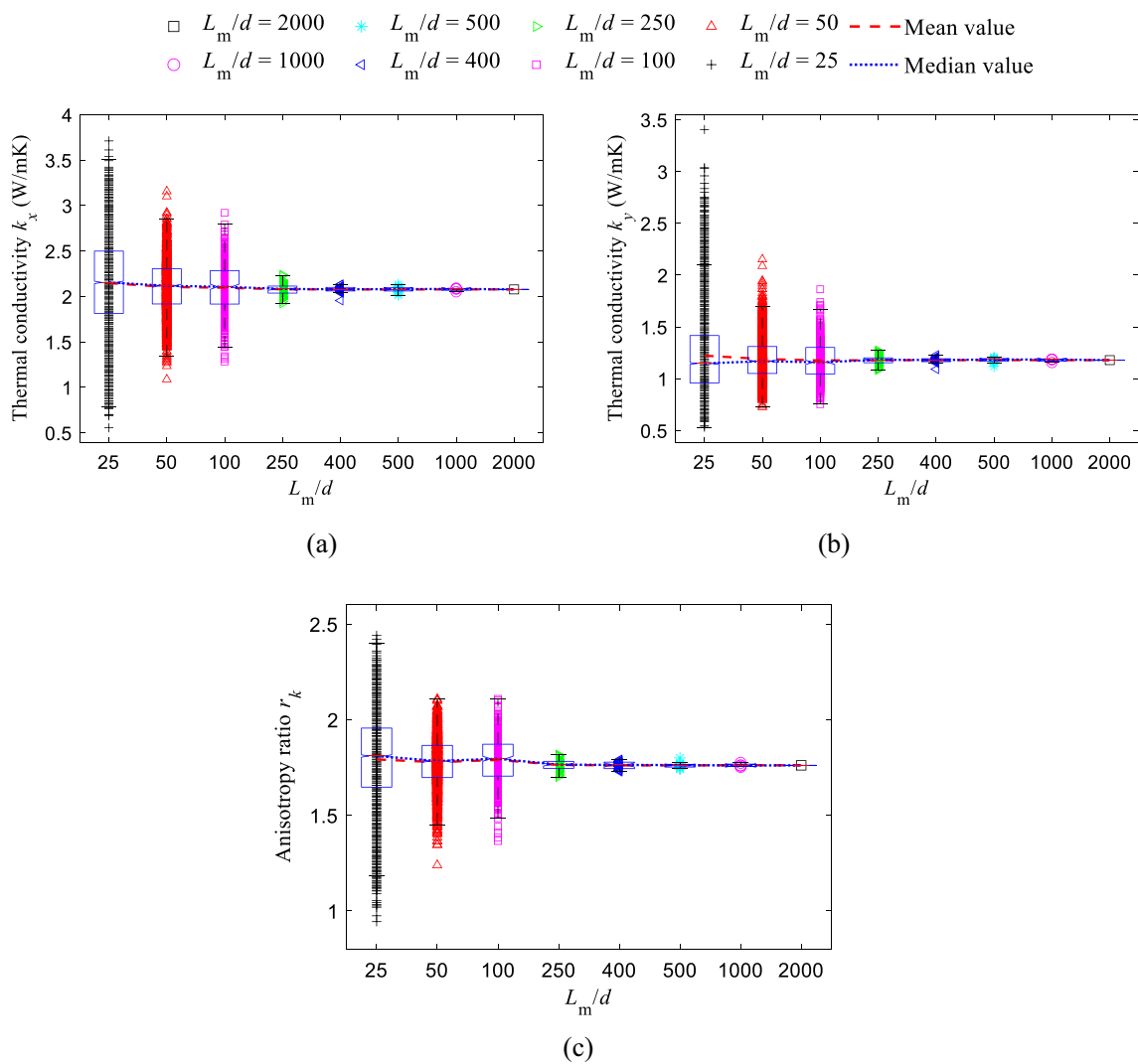


Fig. 8 Box plots of thermal properties of SVE at different scales for geomaterials at saturated state: (a) thermal conductivity k_x ; (b) thermal conductivity k_y ; (c) anisotropy ratio r_k

increases. Notably, the COV of r_k in saturated samples at larger scales is approximately close to 0, while that of dry samples gradually decreases with the increment of the observed scale (see Fig. 9b-1). Therefore, the variation of thermal properties is not negligible when the samples are tested at small scales. To ensure more accurate measurements, it is crucial to have an adequate number of laboratory samples, especially for anisotropic geomaterials with lower moisture content.

Upscaling thermal properties

To evaluate the thermal properties of anisotropic geomaterials at large scales such as metre-scale or kilometre-scale, it is often impractical to perform direct numerical simulations on

the entire sample due to the computational burden. Accordingly, an upscaling scheme can be an efficient tool to calculate thermal properties, which involves simplification strategies to reduce the complexity. In practice, the averaging methods are often applied for upscaling problems. Herein, we considered four averaging models, including arithmetic average model, harmonic average model, geometric average model and quadratic average model, to estimate the thermal properties at a coarse scale by averaging the results from high-resolution grid cells at small scales. The specific expressions of four averaging schemes are shown below.

$$k_A = \sum_{i=1}^n k_i/n \tag{6a}$$

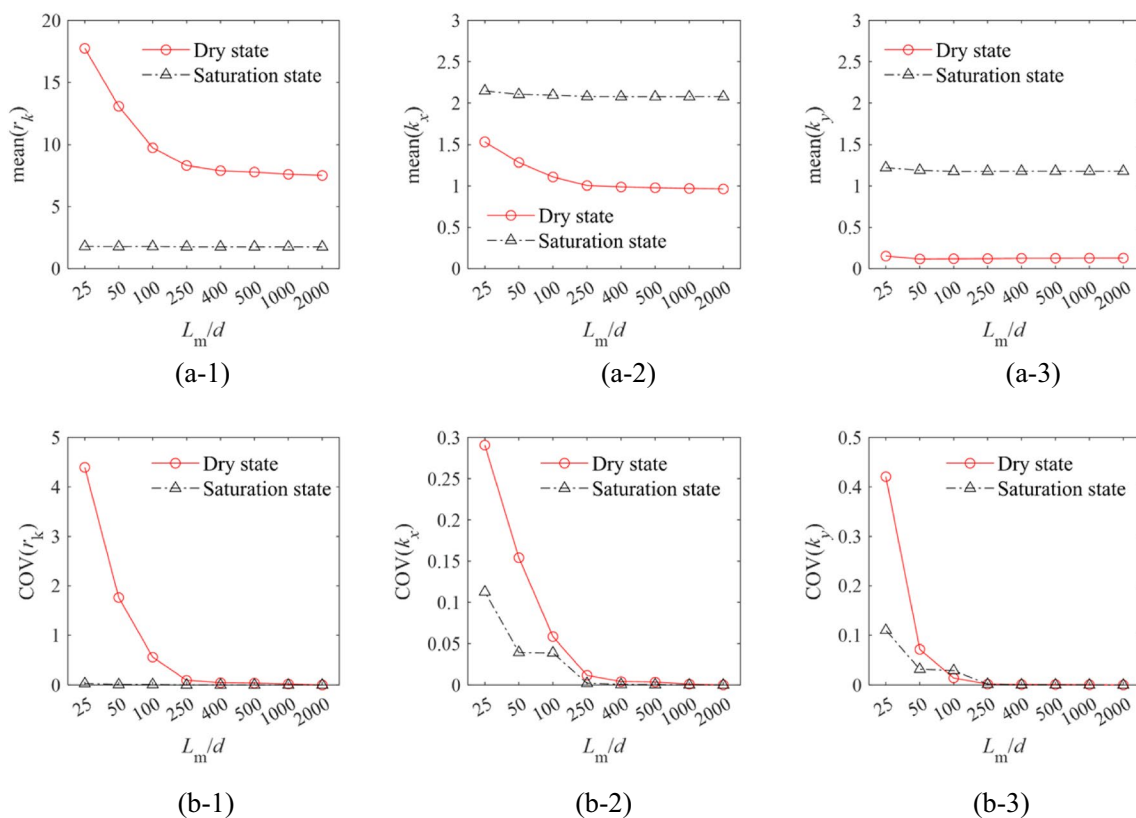


Fig. 9 Statistical results: (a) mean value of thermal properties; (b) COV of thermal properties

$$k_H = n / \sum_{i=1}^n \frac{1}{k_i} \tag{6b}$$

$$k_G = \sqrt[n]{\prod_{i=1}^n k_i} \tag{6c}$$

$$k_Q = \sqrt{\sum_{i=1}^n k_i^2 / n} \tag{6d}$$

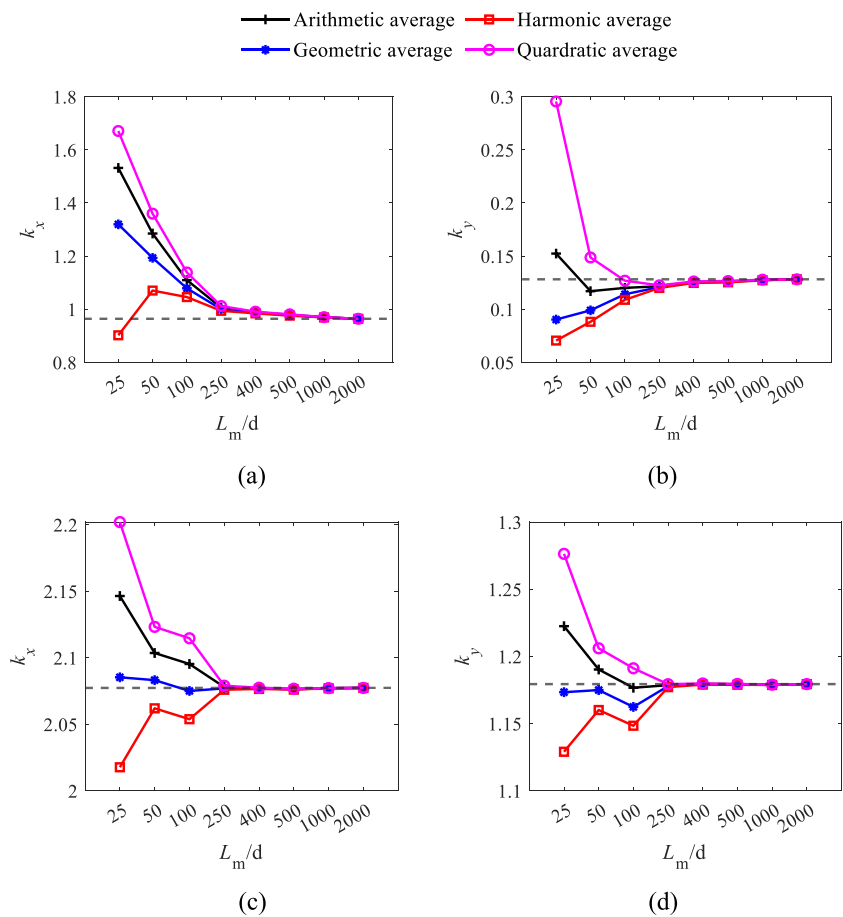
where n is the number of SVE, k_i is the thermal conductivity of i th SVE, k_A is the arithmetic average of SVEs, k_H is the harmonic average of SVEs, k_G is the geometric average of SVEs and k_Q is the quadratic average of SVEs.

The thermal conductivity of sample T is calculated by averaging k of each SVE with various dimensions, and the corresponding results are shown in Fig. 10. It can be noted that the differences between k_x and k_y calculated by four averaging models at dry conditions are larger than that at saturated conditions. The thermal conductivity of geomaterials is affected by the volumetric fraction and individual properties of each component with geomaterials. For dry samples, the pores are filled

with air whose thermal conductivity equals 0.02 W/(mK) (Li et al. 2020). In contrast, the thermal conductivity of water occupying the entire pore space within the saturation sample is 0.5 W/(mK) (Li et al. 2020). Accordingly, for a particular type of geomaterial with the same porosity, the thermal conductivity of the geomaterial at the saturation state is higher than that at the dry condition. It can be observed that the values in Fig. 10c–d are higher than the corresponding values in Fig. 10a–b. Referring to Fig. 9, the COVs of r_k of dry samples are higher than those of saturation samples, which indicates that the values of r_k of SVEs at dry conditions exhibit significant variations. In other words, the deviations between k_x and k_y of SVE are more pronounced. After implementing four averaging schemes, the differences in ultimate average values between k_x and k_y of sample T at dry state are also more remarkable than those for sample T at saturation state, as shown in Fig. 10.

In general, the thermal conductivity of sample T obtained from various averaging methods varies slightly as the dimension of SVE increases, all of which tend to converge to the data calculated by direct FEM. In view of sample T at a dry state, it appears that harmonic average can be used to assess k_x , whereas the arithmetic average model is more suitable for evaluating k_y . As for saturated

Fig. 10 Thermal conductivity of sample *T* calculated by averaging method: (a) k_x at dry state; (b) k_y at dry state; (c) k_x at saturated state; (d) k_y at saturated state. The dashed line denotes the datum calculated by direct FEM



samples, the geometric average nearly coincides with the thermal conductivity from direct FEM over the entire sample *T*. Therefore, the minimum observed size should be limited to 1/8 (=250/2000) size of the macroscale sample of interest to derive relatively accurate results.

The thermal conductivity of geomaterials exhibits inherent anisotropy, although its value may vary at different positions within samples and be dependent on the scale to some extent. This study investigates the anisotropic thermal properties of heterogeneous geomaterials and reveals that thermal conductivity is scale-dependent, particularly for samples with lower moisture content. Notably, significant variations in thermal conductivity are observed at small scales. These variations arise primarily due to the focus of laboratory examinations on relatively small volumes of heterogeneous geomaterials compared to field conditions.

The internal structures of samples at small scales are unique, with notable heterogeneity such as varying porosity. These structural differences strongly impact the thermal properties of the tested samples. Additionally, specific barriers to heat conduction or flow channels with high connectivity play a significant role at smaller scales but gradually diminish in importance as the sample dimensions increase.

It is important to recognise that the data obtained from laboratory measurements reflect local thermal responses and are insufficient to fully capture the actual heat transfer behaviour at larger scales. This limitation stems from the fact that laboratory examinations typically focus on relatively small volumes of heterogeneous geomaterials compared to the scale of field conditions. The complexity of the geomaterials' internal structures and the interplay between different factors at different scales necessitate a more comprehensive understanding of thermal conductivity anisotropy to accurately model and predict heat transfer in real-world scenarios.

Figure 11 demonstrates an upscaling framework to determine the thermal properties of anisotropic geomaterials. It is worth noting that when upscaling the fine-scale (e.g. laboratory-scale) experimental or numerical tests on the geomaterial samples to field scale, the resolution of fine grids should be emphasised. Appropriate resolution selection enables engineers to capture geomaterials' complex internal structures and anisotropic behaviour effectively. Besides, with the aid of approximate upscaling methods, a more accurate representation of the thermal properties at larger scales can be achieved, facilitating reliable predictions and modelling of heat transfer phenomena in real-world applications.

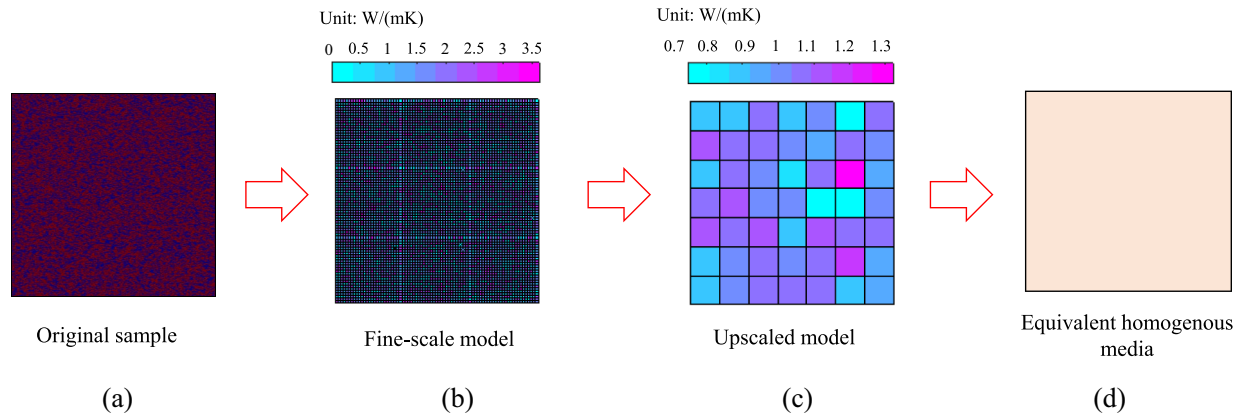


Fig. 11 Upscaling framework for evaluating anisotropy thermal properties of heterogeneous geomaterial

Conclusions

This study focuses on the thermal properties (i.e. thermal conductivity and its anisotropy) of heterogeneous geomaterial. A typical geomaterial sample reconstructed by the QSGS method is regarded as a representativity of in situ sample and decomposed into a series of SVE. The values of thermal conductivity and anisotropy ratio of samples with different dimensions are calculated by FEM to explore the scale dependence of heterogeneous geomaterials. In addition, appropriate and effective upscaling schemes for regional-scale evaluation of properties or geothermal potential are also recommended for references to link the anisotropy of in situ geomaterials and laboratory measurements. The primary conclusions are summarised as follows.

The reconstructed geomaterials by the QSGS method display distinct layered features since most maximum Feret diameters lie vertically, which indicates that the reconstructed sample is a typical representative of heterogeneous geomaterial and can be capable of analysing the scale dependency on the anisotropy of thermal conductivity.

For the dry samples, both the mean values of k_x and r_k have similar decreasing trends with the increment of L_m/d . The mean value of k_y hardly changes with the sample dimension. Unlike dry geomaterials, the discrepancy of mean values of thermal properties between different scales is not as apparent for saturated samples, implying a slight decrease when the sample dimension increases. The thermal behaviours of geomaterials in practice probably lie between the results of two extreme conditions (dry and saturation) of geomaterials.

The anisotropic properties of heterogeneous geomaterials exhibit significant scale dependence, especially the dry geomaterial samples. The values of thermal properties of samples at fine scales become more fluctuant, and their variation gradually decreases to zero with the increment of sample dimension.

Results demonstrated that the samples at small scales are insufficient to manifest the inherent anisotropic thermal conductivity in the field, and directly upscaling the results to a global or regional scale may import errors. For specimens in the laboratory, the experimental scale is capable of determining the thermal conductivity within the mesoscale (i.e. mm and cm) surrounding the sample or a borehole, but it is prone to fail to reflect the actual inherent anisotropy of heterogeneous geomaterials.

The minimum length of refined grids should be limited to 1/8 sample dimension of interest so that four averaging methods can perform well to assess thermal conductivity. For k_x of dry samples, harmonic and arithmetic average models are more suitable for determining k_x and k_y , respectively. In addition, the geometric average model also performs better than the other three averaging methods for saturated geomaterials.

In conclusion, this research presents a novel framework to discuss the scale dependence on the thermal properties of anisotropic geomaterials, which can serve as a reference for the design and analysis of the anisotropic geomaterials in terms of the multi-scale field. However, limited by the lack of available samples of good quality and measured data of r_k for various types of geomaterials, this study is likely not to perfectly replicate a geomaterial specimen with real-world properties but yield a series of statistical analyses with uncertainty qualification to provide a new perspective to explore the scale dependency of anisotropy in thermal conductivity. Besides, this work merely illustrated one typical in situ sample with a relatively high porosity (i.e. 0.5). It would be beneficial to acquire additional field-scale data to validate the effectiveness and applicability of upscaling schemes. Future work stemming from this preliminary study could involve the integration of more available field data representing geostatistical measurements to further narrow the gap between upscaling schemes and real-world energy and environment engineering applications. Moreover,

comprehensive investigations of the influence of porosity on the scale dependency of anisotropy in thermal conductivity will be a focal point of future research.

Symbols a : Empirical parameter; C_d : Distribution probability of solid particle core; d : Minimum scale (i.e. grid cell); k : Thermal conductivity; k_{dry} : Thermal conductivity of geomaterials at dry state; k_{sat} : Thermal conductivity of geomaterials at saturated state; k_p : Thermal conductivity of materials in pore domain; k_x : Effective thermal conductivity along x direction; k_y : Effective thermal conductivity along y direction; K_r : Normalised thermal conductivity; L : Length of macroscale sample; L_m : Length of mesoscale sample; M : Number of SVE that equals to L/L_m ; n : Porosity; P_i : Growth probability of solids along i -direction ($i = 1, 2, 3, 4, 5, 6, 7, 8$); q : Heat flux; r_k : Anisotropy ratio of the thermal conductivity; S_r : Saturation degree; T : Temperature; T_0 : Temperature applied at the boundary; Y : Ratio of P_1 to P_2 ; n : Outward normal vector to the simulation domain; ∇T : Temperature gradient; COV : Coefficient of variation; FEM : Finite element method; $GCHP$: Ground-coupled heat pump; $QSGS$: Quartet structure generation set; RVE : Representative volume element; SVE : Statistical volume element; TRT : Thermal response test

Funding Open Access funding enabled and organized by Projekt DEAL. This research is supported by the National Natural Science Foundation of China (grant No. U22A20596) and International Joint Research Platform Seed Fund Program of Wuhan University (grant No. WHUZZJJ202207). Guan Chen would like to thank the financial support of Sino-German (CSC-DAAD) Postdoc Scholarship Program.

Declarations

Conflict of interest The authors declare no competing interests.

Open Access This article is licensed under a Creative Commons Attribution 4.0 International License, which permits use, sharing, adaptation, distribution and reproduction in any medium or format, as long as you give appropriate credit to the original author(s) and the source, provide a link to the Creative Commons licence, and indicate if changes were made. The images or other third party material in this article are included in the article's Creative Commons licence, unless indicated otherwise in a credit line to the material. If material is not included in the article's Creative Commons licence and your intended use is not permitted by statutory regulation or exceeds the permitted use, you will need to obtain permission directly from the copyright holder. To view a copy of this licence, visit <http://creativecommons.org/licenses/by/4.0/>.

References

- Balland V, Arp PA (2005) Modeling soil thermal conductivities over a wide range of conditions. *J Environ Eng Sci* 4(6):549–558
- Blázquez CS, Martín AF, Nieto IM, García PC, Pérez LSS, Aguilera DG (2017) Thermal conductivity map of the Avila region (Spain) based on thermal conductivity measurements of different rock and soil samples. *Geothermics* 65:60–71
- Brigaud F, Vasseur G (1989) Mineralogy, porosity and fluid control on thermal conductivity of sedimentary rocks. *Geophys J Int* 98(3):525–542
- Buntebarth G (2004) Bestimmung thermophysikalischer Eigenschaften an Opalinustonproben. Geophysikalisch-Technisches Büro, Clausthal-Zellerfeld
- Čermák V, Rybach L (1982) Thermal conductivity and specific heat of minerals and rocks. In: Angenheister G (ed) *Landolt-Börnstein: Numerical data and functional relationships in science and technology*, vol V/1a. Springer, Berlin, pp 305–343
- Cho WJ, Kwon S, Choi JW (2009) The thermal conductivity for granite with various water contents. *Eng Geol* 107(3-4):167–171
- Corcoran A, Eslami-Nejad P, Bernier M, Badache M (2019) Calibration of thermal response test (TRT) units with a virtual borehole. *Geothermics* 79:105–113
- Côté J, Konrad JM (2005) A generalized thermal conductivity model for soils and construction materials. *Can Geotech J* 42(2):443–458
- Côté J, Konrad JM (2009) Assessment of structure effects on the thermal conductivity of two-phase porous geomaterials. *Int J Heat Mass Transf* 52(3-4):796–804
- Dao LQ, Delage P, Tang AM, Cui YJ, Pereira JM, Li XL, Sillen X (2014) Anisotropic thermal conductivity of natural Boom Clay. *Appl Clay Sci* 101:282–287
- Davis MG, Chapman DS, Van Wagoner TM, Armstrong PA (2007) Thermal conductivity anisotropy of metasedimentary and igneous rocks. *J Geophys Res Solid Earth* 112:B05216
- Deming D (1994) Estimation of the thermal conductivity anisotropy of rock with application to the determination of terrestrial heat flow. *J Geophys Res Solid Earth* 99(B11):22087–22091
- Di Sipio E, Galgario A, Destro E, Teza G, Chiesa S, Giaretta A, Manzella A (2014) Subsurface thermal conductivity assessment in Calabria (southern Italy): a regional case study. *Environ Earth Sci* 72:1383–1401
- Elkholy A, Sadek H, Kempers R (2019) An improved transient plane source technique and methodology for measuring the thermal properties of anisotropic materials. *Int J Therm Sci* 135:362–374
- Farouki OT (1981) Thermal properties of soils. Cold Regions Research and Engineering Lab Hanover NH
- Germanou L, Ho MT, Zhang Y, Wu L (2018) Intrinsic and apparent gas permeability of heterogeneous and anisotropic ultra-tight porous media. *J Nat Gas Sci Eng* 60:271–283
- Ghysels G, Benoit S, Awol H, Jensen EP, Debele Tolche A, Anibas C, Huysmans M (2018) Characterization of meter-scale spatial variability of riverbed hydraulic conductivity in a lowland river (Aa River, Belgium). *J Hydrol* 559:1013–1027
- Grubbe K, Haenel R, Zoth G (1983) Determination of the vertical component of thermal conductivity by line source methods. *Zentralblatt für Geologie und Paläontologie Teil 1(1-2):49–56*
- Haffen S, Géraud Y, Rosener M, Diraison M (2017) Thermal conductivity and porosity maps for different materials: a combined case study of granite and sandstone. *Geothermics* 66:143–150
- Han Y, Wang Y, Liu C, Hu X, An Y, Du L (2023) Study on thermal conductivity of non-aqueous phase liquids-contaminated soils. *J Soils Sediments* 23(1):288–298
- Hill R (1963) Elastic properties of reinforced solids: some theoretical principles. *J Mech Phys Solids* 11(5):357–372
- Huang XW, Guo J, Li KQ, Wang ZZ, Wang W (2023) Predicting the thermal conductivity of unsaturated soils considering wetting behavior: a meso-scale study. *Int J Heat Mass Transf* 204:123853
- Johansen. (1977) Thermal conductivity of soils. Cold Regions Research and Engineering Lab, Hanover NH
- Jorand R, Vogt C, Marquart G, Clauser C (2013) Effective thermal conductivity of heterogeneous rocks from laboratory experiments and numerical modeling. *J Geophys Res Solid Earth* 118(10):5225–5235
- Journal AG, Huijbregts CHJ (1978) Mining geostatistics. Academic Press Inc., London, UK
- Jung J, Demeke W, Lee S, Chung J, Ryu B, Ryu S (2021) Micromechanics-based theoretical prediction for thermoelectric properties of anisotropic composites and porous media. *Int J Therm Sci* 165:106918
- Lake LW (1988) The origins of anisotropy (includes associated papers 18394 and 18458). *J Pet Technol* 40(04):395–396

- Li KQ, Chen G, Liu Y, Yin ZY (2023c) Scale effect on the apparent anisotropic hydraulic conductivity of geomaterials. *ASCE-ASME J Risk Uncertain Eng Syst, Part A: Civil Eng* 9(3):04023020
- Li KQ, Li DQ, Liu Y (2020) Meso-scale investigations on the effective thermal conductivity of multiphase materials using the finite element method. *Int J Heat Mass Transf* 151:119383
- Li KQ, Liu Y, Yin ZY (2023b) An improved 3D microstructure reconstruction approach for porous media. *Acta Mater* 242:118472
- Li KQ, Miao Z, Li DQ, Liu Y (2022) Effect of mesoscale internal structure on effective thermal conductivity of anisotropic geomaterials. *Acta Geotech* 17:3553–3566
- Li KQ, Yin ZY, Liu Y (2023a) Influences of spatial variability of hydrothermal properties on the freezing process in artificial ground freezing technique. *Comput Geotech* 159:105448
- Liu Y, Li KQ, Li DQ, Tang XS, Gu SX (2022) Coupled thermal-hydraulic modeling of artificial ground freezing with uncertainties in pipe inclination and thermal conductivity. *Acta Geotech* 17(1):257–274
- Mehmani Y, Burnham AK, Tchelepi HA (2016) From optics to upscaled thermal conductivity: Green River oil shale. *Fuel* 183:489–500
- Midttømme K, Roaldset E (1998) The effect of grain size on thermal conductivity of quartz sands and silts. *Pet Geosci* 4(2):165–172
- Midttømme K, Roaldset E, Aagaard P (1997) Thermal conductivities of argillaceous sediments. *Geol Soc, London, Eng Geol Spec Publ* 12(1):355–363
- Midttømme K, Roaldset E, Aagaard P (1998) Thermal conductivity of selected claystones and mudstones from England. *Clay Miner* 33(1):131–145
- Mitchell JK, Soga K (2005) *Fundamentals of soil behavior*, third edn. John Wiley & Sons, Inc.
- Mügler C, Filippi M, Montarnal P, Martinez JM, Wileveau Y (2006) Determination of the thermal conductivity of opalinus clay via simulations of experiments performed at the Mont Terri underground laboratory. *J Appl Geophys* 58(2):112–129
- Nie J, Cui Y, Senetakis K et al (2023) Predicting residual friction angle of lunar regolith based on Chang'e-5 lunar samples. *Sci Bull* 68(7):730–739
- Nie JY, Zhao JD, Cui YF, Li DQ (2021) Correlation between grain shape and critical state characteristics of uniformly graded sands: a 3D DEM study. *Acta Geotech* 17:2783–2798
- Penner E (1963) Anisotropic thermal conduction in clay sediments. *Proc Int Clay Conference Stockholm* 1:365–376
- Popov Y, Beardmore G, Clauser C, Roy S (2016) ISRM suggested methods for determining thermal properties of rocks from laboratory tests at atmospheric pressure. *Rock Mech Rock Eng* 49:4179–4207
- Popov YA, Pribnow DF, Sass JH, Williams CF, Burkhardt H (1999) Characterization of rock thermal conductivity by high-resolution optical scanning. *Geothermics* 28(2):253–276
- Prats M, O'Brien SM (1975) The thermal conductivity and diffusivity of Green River oil shales. *J Pet Technol* 27(01):97–106
- Rapti D, Marchetti A, Andreotti M, Neri I, Caputo R (2022) GeoTh: an experimental laboratory set-up for the measurement of the thermal conductivity of granular materials. *Soil Systems* 6(4):88
- Rodriguez-Dono A, Zhou Y, Olivella S (2023) A new approach to model geomaterials with heterogeneous properties in thermo-hydro-mechanical coupled problems. *Comput Geotech* 159:105400
- Samadhiya NK, Viladkar MN, Al-Obaydi MA (2008) Numerical implementation of anisotropic continuum model for rock masses. *Int J Geomech* 8(2):157–161
- Schön JH (1996) *Physical properties of rocks: fundamentals and principles of petrophysics*. Elsevier, Oxford
- Tarnawski VR, McCombie ML, Momose T, Sakaguchi I, Leong WH (2013) Thermal conductivity of standard sands. Part III. Full range of saturation. *Int J Thermophys* 34:1130–1147
- Vasseur G, Brigaud F, Demongodin L (1995) Thermal conductivity estimation in sedimentary basins. *Tectonophysics* 244(1-3):167–174
- Walton WH (1948) Feret's statistical diameter as a measure of particle size. *Nature* 162(4113):329–330
- Wang J, Carson JK, North MF, Cleland DJ (2006) A new approach to modelling the effective thermal conductivity of heterogeneous materials. *Int J Heat Mass Transf* 49(17-18):3075–3083
- Wang M, Wang J, Pan N, Chen S (2007) Mesoscopic predictions of the effective thermal conductivity for microscale random porous media. *Phys Rev E* 75(3):036702
- Wang Z, Xin L, Xu Z, Shen L (2017) Lattice Boltzmann simulation of heat transfer with phase change in saturated soil during freezing process. *Numer Heat Transf, Part B: Fundam* 72(5):361–376
- Yang Z, Nie J, Peng X, Tang D, Li X (2021) Effect of random field element size on reliability and risk assessment of soil slopes. *Bull Eng Geol Environ* 80:7423–7439
- Yu H, Lu C, Liu W, Chen W, Li H, Huang J (2023) Anisotropic thermal properties of an argillaceous rock under elevated temperatures and external load conditions. *Case Stud Therm Eng* 42:102724
- Zhang F, Cui YJ, Zeng L, Conil N (2019) Anisotropic features of natural Teguline clay. *Eng Geol* 261:105275
- Zhang JZ, Zhang DM, Huang HW, Phoon KK, Tang C, Li G (2022) Hybrid machine learning model with random field and limited CPT data to quantify horizontal scale of fluctuation of soil spatial variability. *Acta Geotech* 17:1129–1145
- Zhou Y, Yan C, Tang AM, Duan C, Dong S (2019) Mesoscopic prediction on the effective thermal conductivity of unsaturated clayey soils with double porosity system. *Int J Heat Mass Transf* 130:747–756